SIZE EFFECTS FOR THE STRENGTH OF CERAMIC TILES

L.J.M.G. Dortmans*, Z. Gao**, G. de With** and A. Reymer*

* TNO Institute of Applied Physics
P.O. Box 595, 5600 AN Eindhoven, the Netherlands
** Eindhoven University of Technology
P.O. Box 513, 5600 MB Eindhoven, the Netherlands

ABSTRACT

Strength measurements were carried out on a class BI ceramic tile using 3-point bend and ball-on-ring tests with different specimen sizes and support conditions. The variation in strength can be characterized by means of a Weibull distribution with a Weibull modulus of about 15 and a mean strength depending on the effective volume V_{eff} of the test. This dependency cannot be described with standard weakest-link fracture models. A modified model is proposed which has previously been formulated to describe the similar anomalous statistical behaviour of advanced technical ceramics.

1. INTRODUCTION

Fracture due to contact loading is an important life-time limiting aspect for ceramic floor tiles. Methods to describe and predict fracture due to localized contact stresses are therefore considered as a valuable tool, e.g. for design studies in which weight (thickness) reduction and the influence of the stiffness of the foundation are considered.

To arrive at such a tool, the strength of a floor tile as a function of geometry and loading conditions has to be analyzed first. To this purpose, mechanical tests were carried out on a single type of floor tile (class BI). These tests were carried out to establish whether the well-known size effect as found for advanced technical ceramics (in which strength depends on the tested volume), is also observed for these materials. The tests contained 3-point bend tests and ball-on-ring tests on differently sized specimens. The results of these tests were interpreted using a weakest-link statistical strength model, allowing for a description of the variation of strength with specimen size and loading conditions.

2. MATERIAL AND METHODS

The ceramic tile used is a class BI tile as obtained from the manufacturer. All tiles were processed in a single batch and had nominal dimensions of 295 x 295 x 7.5 mm. From these tiles suitable test pieces were obtained by sawing and grinding. The glaze layer of the tile was not removed by grinding because testing was done in such a way that the relevant maximum tensile stress in the bend tests always was near the ground surface of the specimen, where fracture originated. In these conditions the influence of the relatively thin glaze layer is believed to be negligible [1]. Grinding was performed to remove any surface irregularities due to the pressing procedure from the loaded surface, resulting in a typical surface roughness R_a of about 1 μm.

For the 3-point bend tests [2] the specimen sizes and support conditions given in Table I apply.

test	specimen length L [mm]	support span S [mm]	specimen width W [mm]	specimen thickness H [mm]	Mean fracture stress S_{mf} [MPa]
1	150	100	30	7.35	68.5
2	250	200	30	7.35	64.6
3	50	36	20	3.05	73.5
4	50	36	20	5.00	72.0
5	50	36	20	7.50	71.1
6	50	20	20	3.05	69.5
7	50	20	20	5.00	71.8
8	50	20	20	7.50	70.3

Table I: Specimen sizes, support conditions and mean fracture stress for 3-point bend tests.

The fracture toughness of the material was determined using a Single Edge Notched Beam specimen (W=10 mm, H=7.5 mm, notch length 2.0 mm, notch width 120 μm) loaded in 3-point bending with a support span S of 30 or 60 mm [11].

The ball-on-ring tests [2] were carried out on the specimen as specified in table II. The diameter of the hardened steel loading ball was 15 mm.

test	specimen diameter [mm]	support diameter [mm]	specimen thickness [mm]	mean fracture stress S_{mf} [MPa]
9	48	30	3.00	76.1
10	48	30	5.05	75.7
11	48	30	7.30	79.9
12	78	60	3.05	73.2
13	78	60	5.05	71.4
14	70	60	7.30	73.8
15	100	78	7.40	74.1

Table II: Specimen sizes, support conditions and mean fracture stress for ball-on-ring tests.

All tests were carried out on a universal testing machine at room temperature in dry nitrogen gas with a dewpoint $\leq$ -25 °C.

3. TEST RESULTS

3.1 Strength tests

The tests 1 to 15 given in tables I and II were carried out on 20 to 40 test pieces for each test. From the measured fracture force the maximum principal stress S_f at the tensile loaded surface can be computed. The mean value for S_f, S_{mf}, for each test is as given in tables I and II. These results clearly show a size dependent strength with extreme values of 64.6 (test 2) and 79.9 (test 11) MPa. The scatter in strength can be characterized by applying a weakest-link (Weibull) statistical model in which the failure probability P_f is expressed as

$$P_f = 1 - \exp[-(S_f/S_o)^m] \qquad (1)$$

with S_o as a geometry dependent scale parameter and m as the Weibull modulus. Figure 1 shows a typical result of plotting experimental data according to the linearized version of the above equation (Weibull plot)

$$\ln(\ln(1/(1-P_f)) = m \ln(S_f) - m \ln(S_o) \qquad (2)$$

Using a maximum likelihood method the parameter m can be determined from the strength data [3]. A typical value of m of 15 is then obtained. The scatter in the Weibull modulus is about 3 which is consistent with the expected scatter $m/\sqrt{N}$ [3] with N as the number of test pieces in a test.

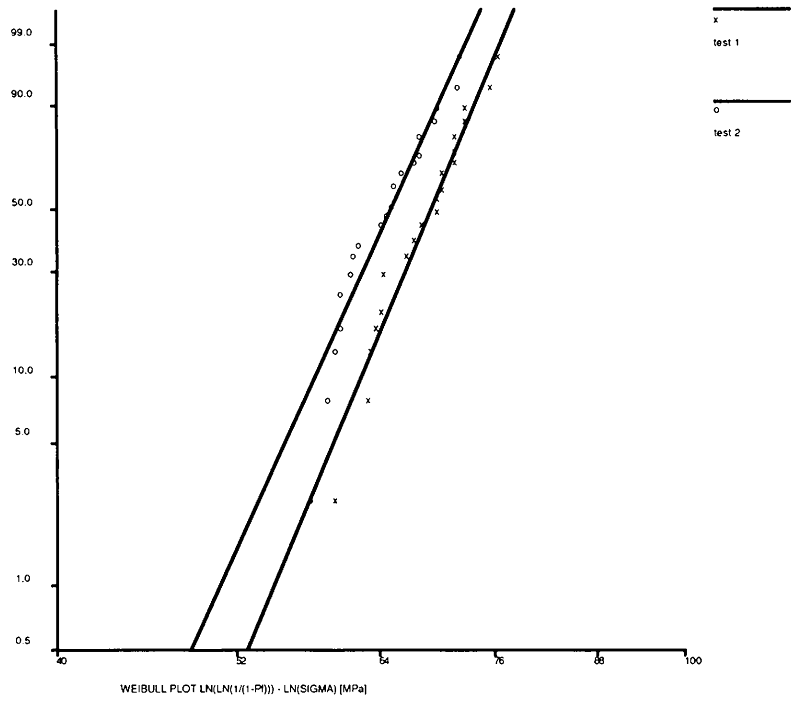

Figure 1: Weibull plot for tests 1 and 2.

3.2 Fracture toughness tests

The fracture toughness determined on 5 samples amounted 1.61 (0.07) and 1.63 (0.05) $MPa\sqrt{m}$ for the support span of 30 and 60 mm respectively, where the numbers in brackets indicate the sample standard deviation. The average value for K_{Ic} of 1.62 $MPa\sqrt{m}$ and a typical strength value S_{mf} of 75 MPa (tables I and II) result in a typical critical defect size a_{cr} of about 300 µm according to the Griffith equation $K_{ic} = Y\ S_{mf} \sqrt{a_{cr}}$ with Y = 1.26 for half penny shaped surface defects. Defects of this size can be pores or porely sintered agglomerates, as were observed in the microstructure of the material via optical and scanning electron microscopy.

4. STRENGTH MODELLING

To model the strengh variation for the different tests a weakest-link statistical model can be applied [4,5,6]. Standard weakest-link fracture models predict that the mean fracture stress S_{mf} is given by

$$S_{mf} = S_u\ (V_u\ /\ V_{eff})^{1/m} \qquad (3)$$

Here S_u is the geometry independent strength per unit volume $V_u = 1\ mm^3$ and V_{eff} is the so-called effective volume. The value of V_{eff} can be determined by proper integration of the stress field in the test piece, employing a chosen fracture model and the Weibull modulus m [6]. For the fracture model various options are given in literature, e.g. Principle of Independent Action (PIA, [8]), Normal Stress Averaging (NSA, [9]) and Maximum Strain Energy Release Rate (GMAX, [10]). In this paper only the PIA model is discussed further because the other fracture models turned out to give less accurate results in terms of correlation coefficients. The required integration to obtain the effective volume V_{eff} was carried using a special postprocessor FAILV3 [4,6] to a commercial Finite Element package. Figure 2 shows the dependence of S_{mf} on $(1/V_{eff})^{1/m}$ for the PIA fracture model where V_{eff} ranges from 0.48 for test 9 to 166 for test 2. The solid line in Figure 2 represents the standard weakest-link dependency given in equation (3). Because of the relatively high value of 15 for the Weibull modulus m, the variation in strength with V_{eff} is not very large, but still significant. Obviously the dependency according to the standard model (3) is not satisfactory: significant deviations occur. These deviations are considered relevant as the expected standard deviation in the mean strength S_{mf} for an individual test is given by $S_{mf}/m\sqrt{N}$ [4]. With m=15, the number of specimens N taken typically 20 and S_{mf} typically 75 MPa, the standard deviation is about 1 MPa. This is much smaller than the deviations (maximum about 9 MPa) from the standard model (3) observed in Figure 2.

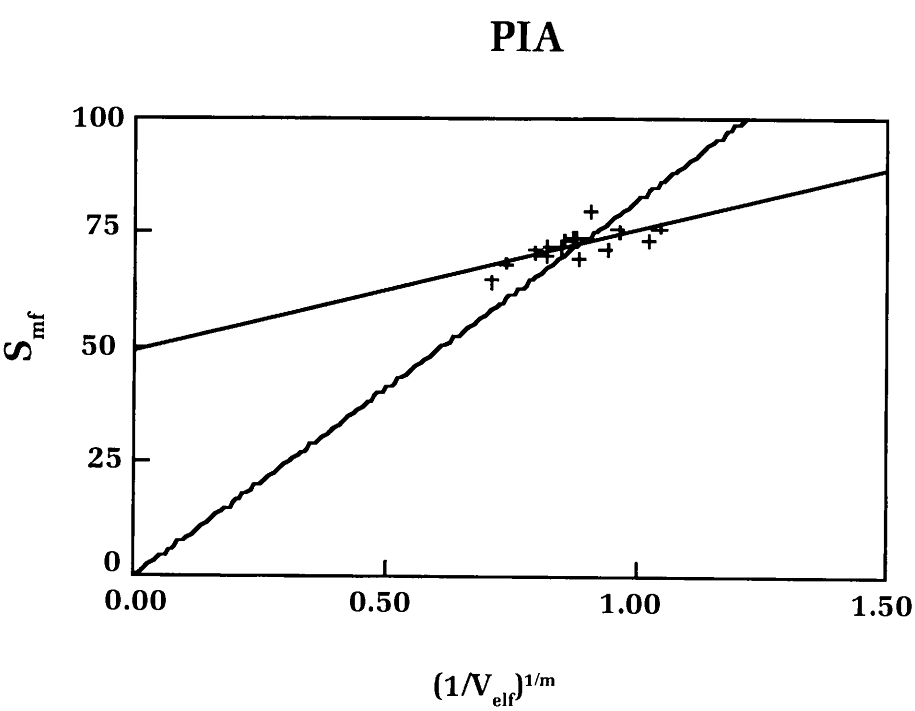

Figure 2: S_{mf} versus $(1/V_{eff})^{1/m}$ for the PIA fracture model. The solid line is according to equation (3), the dashed line is according to the anomalous statistical model by Scholten et al. [7] (equation (4)).

These findings are similar to the observations of Scholten et al. [7] on the size effect of various advanced technical ceramics where also an anomalous behaviour was observed. The conclusion is that the size effect law (3) is not valid. Scholten et al. [7] have modelled this anomalous behaviour by fitting the data to a linear dependency as given by the dashed line in Figure 2 which is given by the equation

$$S_{mf} = S_r + S_u \,(1/V_{eff})^{1/m}) \qquad (4)$$

with S_r = 49.4 MPa and S_u = 26.2 MPa. Within the range of values for V_{eff} a dependence as given by equation (4) is considered adequate. For extrapolation to lower or higher values of V_{eff} other models might be considered, but these will be difficult to quantify with experimental data. Large values for V_{eff} are not easily obtained as an upperbound for V_{eff} for a floor tile of the dimensions 295x295x7.5 mm is 1.3×10^6 mm^3 ($(1/V_{eff})^{1/m}$ = 0.39) if the entire tile is equibiaxially loaded in tension. However, such experiments are not easily performed. If bend tests are used a significantly lower value of V_{eff} will always result, partly because of the relatively high value of the Weibull modulus m. Similarly much smaller values of V_{eff} are not easily obtained in experiments. Therefore the range of values for V_{eff} given in Figure 2 is not easily extended and a description as given by equation (4) is considered quite adequate.

5. CONCLUSIONS

Strength measurements were carried out on a class BI ceramic tile using 3-point bend and ball-on-ring tests with different specimen sizes and support conditions. The variation in strength can be characterized by means of a Weibull distribution with a Weibull modulus of about 15 and a mean strength depending on the effective volume V_{eff} of the test. This dependency cannot be described by standard weakest-link fracture models, as was also observed for advanced technical ceramic materials by Scholten et al. [7]. The anomalous size effect observed can be represented using a modified weakest-link model in which the Principle of Independent Action (PIA) is applied and the strength per unit volume depends on specimen size and loading conditions through the effective volume V_{eff} (equation (4)). As a result the mean fracture strength will increase with decreasing V_{eff}, but not as significantly as predicted by the standard model (3).

An explanation for this deviating behaviour could be that for small effective volumes no longer sufficient material is subjected to high stresses to assure that a representative part of material is tested. Weakest-link fracture models are based on this assumption because a key factor in their formulation is the presence of a homogeneously loaded Representative Volume Element (RVE) from which brittle fracture originates. Whether this is a justified explanation is topic for further research.

6. REFERENCES

1- L. Esposito, G. Timellini and A. Tucci, Fracture toughness of traditional ceramic materials: a first approach, Proceedings Fourth Euro Ceramics, vol. 11, pp. 221-230, ed. C. Palmonari, Gruppo Editoriale Faenza Editrice S.p.A., Italy.

2- H. Scholten, L. Dortmans, G. de With, B. de Smet and P. Bach, Weakest-Link Failure Predictions for Ceramics II: Design and Analysis of Uniaxial and Biaxial Bend Tests, Journal of the European Ceramic Society, 10 (1992), 33-40.

3- L. Dortmans and G. de With, Noise sensitivity of fit procedures for Weibull parameter extraction, Journal of the American Ceramic Society, 74 (1991), 2093-2094.

4- L. Dortmans and G. de With, Weakest-link failure prediction for ceramics using finite element postprocessing, Journal of the European Ceramic Society, 8 (1990), 369-374.

5- L. Dortmans and G. de With, Weakest-Link Failure Predictions for Ceramics IV: Application of Mixed-Mode Fracture Criteria for Multiaxial Loading, Journal of the European Ceramic Society, 10 (1992), 109-114.

6- L. Dortmans, Th. Thiemeier, A. Brückner-Foit and J. Smart, WELFEP: A round robin for weakest-link finite element postprocessors, Journal of the European Ceramic Society, 11 (1993), 17-22.

7- H. Scholten, L. Dortmans and G. de With, Application of mixed-mode fracture criteria for weakest-link failure prediction for advanced technical ceramics; In: ASTM STP 1201: Life prediction methodologies and data for ceramic materials , eds. C. Brinkman and S. Duffy, 1993, pp. 192-206.

8- P. Stanley, H. Fessler and A. Sevill, An engineers approach to the prediction of failure probability prediction of brittle components, Proceedings British Ceramic Society, 22 (1973), 453-487.

9- W. Weibull, A statistical theory for the strength of materials, Ingeniors Vetenskaps Akadamien Handlingar, no. 151, 1939.

10- T. Hellen and W. Blackburn, The calculation of stress intensity factors for combined tensile and shear loading, International Journal of Fracture, 10 (1974), 305-321.

11- J. Srawley, Wide range stress intensity factor expressions for ASTM E399 standard fracture toughness specimens, International Journal of Fracture Mechanics, 12 (1976), 475-476.